

Comparison of the sensitivity of two Intelligent Optimization Methods to the uncertainty of the LVAD system parameters in artificial heart

Majid Neshat Yazdi ¹, Reihaneh Kardehi Moghaddam ²

¹Department of Electrical Engineering, Ahar Branch, Islamic Azad University, Ahar, Iran.

Email: M-neshat@iau-ahar.ac.ir

²Department of Electrical Engineering, mashhad branch, Islamic Azad university, mashhad, Iran.

Email: R_k_moghaddam@mshdiau.ac.ir

Abstract

Artificial is usually used by heart failure patients with left ventricular failure. Than those where the disease is left ventricular failure, the most common heart disease in recent years is the other auxiliary equipment for the human heart than considered and used. In this paper, for the first time, the uncertainty of the parameters of the system is considered and the range of stabilized parameter uncertainty which return control feedback to the stabilization of the system is calculated. The sensitivity of optimization algorithms to the uncertainties of system parameters are compared and evaluated. The cost function used was based on the model and control method of sampling the pump and the combined statements of speed fluctuation and output functions of the initial cost is presented. In simulation, the effect of controlling these two methods and Akfa sensitivity to parameter changes is compared.

Key words: current sampling, genetic algorithm, optimization, particle swarm, sensitivity, uncertainty

{**Citation:** Majid Neshat Yazdi, Reihaneh Kardehi Moghaddam. Comparison of the sensitivity of two Intelligent Optimization Methods to the uncertainty of the LVAD system parameters in artificial heart. American Journal of Research Communication, 2013, 1(11): 314-332} www.usa-journals.com, ISSN: 2325-4076.

1. Introduction

The results show that cardiovascular disease is the major cause of death in men and women worldwide [1]. Heart failure is a progressive and chronic disease that its symptoms and effects lead to some limitations in the patients' normal life and affect their life quality over time [2]. Realistic prosthetic heart of the current model, the drawbacks such as large size, short lifespan, the different shape of the pulse, blood pressure, battery problems, blood clots, which appear to be rejected [3]. LVAD can be used for: 1- No need for removal of normal heart when using LVAD, 2- the proper function of the right ventricle in most cases, 3- not to interfere of normal heart rate, 4- Convenient control of physiological conditions, 5- possibility of retrieving heart naturally after using LVAD, 6- convenience, low cost and high reliability of LVAD, 7- using normal heart function as a backup in case of LVAD failure [4]. To increase the efficiency of LVAD, it is the consumption of an energy source that reduces noise and increases accuracy of this system [5]. So far, efforts have been made to improve the performance of the LVAD [6]. In 2005, conditions of a cardiovascular system combined with the pump was provided in a model. The purpose of this model was achieving more stability in design, increasing the controllability of pump speed and providing a model to simulate this system [7]. In [8], modeling, parameters estimation and control of cardiovascular system also was carried by LVAD in which a PI controller with a cost function and three parameters of cardiac output, arterial pressure and left atrium pressure were used. In another article the optimal control of the LVAD provided and the cost of the membership function, including infarct volume, mean left atrial pressure, MV aorta and Average speed pumps were tested, the objective is to minimize changes in function and speed pumps using the circulatory model [9]. The new model was introduced in 2011 LVAD based on biopsy was underway. Combining the previous controllers was very effective in improving the process of

control [10]. However, these methods have limitations such as non-linear changes in flow rate, pump speed fluctuations due to heart rate etc. And there is a vast need of improving the controlling process. In this paper, we examine the impact of uncertainty on the stability of the system. We should firstly mention the previous papers mentioning the uncertainties including sliding controllers, adaptive controllers and robust controllers [11]. According to the second part of the paper, we will address the current state-based modeling and dynamical equations derived in section 3 the effect of uncertain parameters will be studied. In Section 4, the maximum range of uncertainties will be investigated. Multiplicative and additive uncertainties will be described in Section 5 to determine the range of parameters stability finally using genetic algorithm and particle swarm, the optimal controller is carried out in 6.

2. System modeling

Pump picture can be seen in Figure 1. The system has a stator and a rotor.

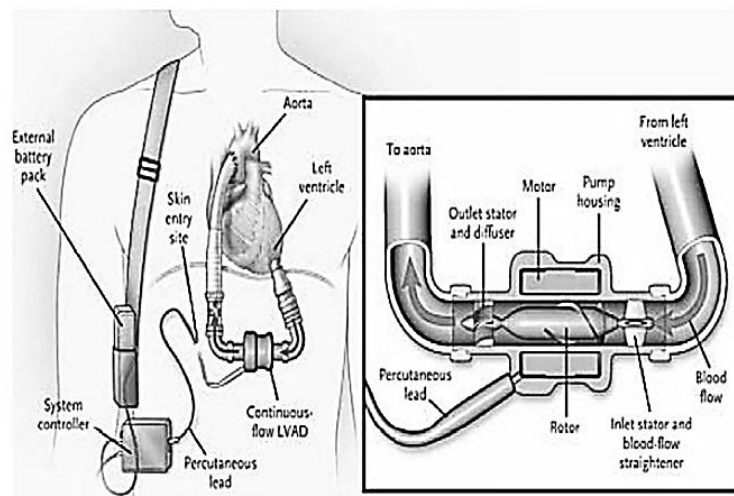


Figure 1: Inside the pump.

Cardiovascular system and the model obtained by combining LVAD can be extracted from the functional model, shown in Figure 2 [10].

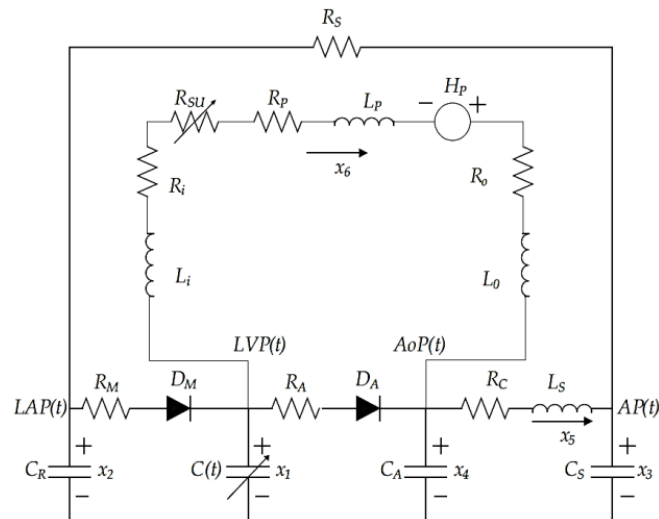


Figure 2: Model of combined cardiac and LVAD.

3. Extraction of the model’s dynamical equations

For aortic and mitral valves which are modeled by D_M and D_A diodes models, there have been several cases which are mentioned in Table 1.

Table 1 - State of the valve within a heart cycle

Modes	Valves		Phases
	Mitral	Aortic	
1	Closed	Closed	Isovolumic Relaxation
2	Open	Closed	Filling
1	Closed	Closed	Isovolumic Contraction
3	Closed	Open	Ejection
-	Open	Open	Not feasible

Using system variables in Table 2, the state space model is expressed in equation (1) [10].

Table 2 - Variables circulatory state of the left ventricle model

Variables	Name	Physiological meaning (units)
X ₁ (t)	LVP(t)	Left ventricular pressure (mmHg)
X ₂ (t)	LAP(t)	Left atrial pressure (mmHg)
X ₃ (t)	AP(t)	arterial pressure (mmHg)
X ₄ (t)	AoP(t)	aortic pressure (mmHg)
X ₅ (t)	Q _T (t)	Total flow (ml/s)
X ₆ (t)	Q _P (t)	Pump flow (ml/s)

$$(1) \begin{bmatrix} \dot{x}_1 \\ \dot{x}_2 \\ \dot{x}_3 \\ \dot{x}_4 \\ \dot{x}_5 \\ \dot{x}_6 \end{bmatrix} = \begin{bmatrix} \frac{-C(t)}{C(t)} & 0 & 0 & 0 & 0 & \frac{-1}{C(t)} \\ 0 & \frac{-1}{R_S C_R} & \frac{1}{R_S C_R} & 0 & 0 & 0 \\ 0 & \frac{1}{R_S C_S} & \frac{-1}{R_S C_S} & 0 & \frac{1}{C_S} & 0 \\ 0 & 0 & 0 & 0 & \frac{-1}{C_A} & \frac{1}{C_A} \\ 0 & 0 & \frac{-1}{L_S} & \frac{1}{L_S} & \frac{-R_S}{L_S} & 0 \\ \frac{1}{L^P} & 0 & 0 & \frac{-1}{L^P} & 0 & \frac{-R^P}{L^P} \end{bmatrix} \begin{bmatrix} x_1 \\ x_2 \\ x_3 \\ x_4 \\ x_5 \\ x_6 \end{bmatrix} + \begin{bmatrix} \frac{1}{C(t)} & \frac{-1}{C(t)} \\ \frac{-1}{C_R} & 0 \\ 0 & 0 \\ 0 & \frac{1}{C_A} \\ 0 & 0 \\ 0 & 0 \end{bmatrix} \begin{bmatrix} \frac{1}{R_M} \Gamma(x_2 - x_1) \\ \frac{1}{R_A} \Gamma(x_1 - x_4) \end{bmatrix} + \begin{bmatrix} 0 \\ 0 \\ 0 \\ 0 \\ 0 \\ \frac{Y}{L^P} \end{bmatrix} \Gamma(t)$$

The numerical values of the parameters of equation (1) are presented in Table (3).

Table 3- Model parameters

Parameters	Value	Physiological meaning
Resistances(mmHg.s/ml)		
R _S	1	Systemic Vascular Resistance
R _M	0.005	Mitral Valve Resistance
R _A	0.001	Aortic Valve Resistance
R _C	0.0398	Characteristic Resistance
R _i	0.0677	Inlet Cannula Resistance
R _P	0.1707	Pump Resistance
R _o	0.0677	Outflow Cannula Resistance
Compliances (ml/mmHg)		
C(t)	Time-varying	Left Ventricular Compliance
C _R	4.4	Left Atrial Compliance
C _S	1.33	Systemic Compliance
C _A	0.08	Aortic Compliance
Inertances (mmHg.s ² /ml)		
L _S	0.0005	Inertance of blood in Aorta
L _i	0.0127	Inlet Cannula Inertance
L _P	0.02177	Pump Inertance
L _o	0.0127	Outflow Cannula Inertance

In relation (1), $r(\xi)$ denotes the ramp function which is calculated in equation (2). The constant parameter of γ is dependent on the pump conversion coefficient, feed voltage and pump efficiency. Values R^* and L^* are expressed as equations (3) and (4). R_{su} is the time-variable non-linear resistance and expressed in equation (5). α depends on the scaling factor and \bar{x}_1 shows the suction rate.

$$(2) \quad r(\xi) = \begin{cases} \xi & \text{if } \xi \geq 0 \\ 0 & \text{if } \xi < 0 \end{cases}$$

$$(3) \quad R^* = R_i + R_o + R_p + R_{su}$$

$$(4) \quad L^* = L_i + L_o + L_p$$

$$(5) \quad R_{su} = \begin{cases} 0 & \text{if } LVP(t) > \bar{x}_1 \\ \alpha(LVP(t) - \bar{x}_1) & \text{if } LVP(t) \leq \bar{x}_1 \end{cases}$$

Although the LVAD system has a high reliability, patients should be still under caring because of long-term unreliability against the changes of patient's body and environmental conditions. This means that, the optimum may be changed during the time and one should reoptimize the system. The reoptimization is so necessary in the controlling process of sensitive systems such as LVAD. In equation (1), there are several parameters which are referred to in table (3). Is referred to, all resistances, R_S , R_M , R_A , R_C , R_i , R_o may change with environmental conditions. For example, increasing the mobility of humans lead to heart rate increase which changes the value of resistance R_M and R_A , heart rate and the change in resistance R_S is, as seen in table (3) R_S one. In this case, the ideal is considered the heart of a patient's resistance to change. These changes affect the resistance R_i and R_o pump are the pump itself is also resistant to indicate that the table (3) the R_p is shown, the other factors can be concentration, blood pressure, glucose blood, age, weight, heat, moisture, and... Noted. To examine the sensitivity of the system to resist changes in R^* is considered. This resistance includes the resistance R_i , R_o , R_p , R_{su} is in

equation (3) is observed. The model has a linear behavior to the uncertainties, but in some cases, the system may be oscillating that may lead to the system interference. This article examines the LVAD system optimization with uncertainty for the first time that may be an evolution in the system. The control targets have been determined according to the importance of the system's response rate and the settling time in controlling the blood pressure with the minimum overshoot and undershoot and using the minimum aortic possible pressure and the left Ventricular to decrease the damage. According to changes of biological parameters in different human activity conditions such as resting, exercising and daily activities, the mean pump speed have to be at the optimum state to bear the minimum energy consumption with the maximum efficiency, since the suction over-speed for a short period of time may stop the Ventricular and damage the heart muscle. According to the importance of the blood volume and its direct proportion with brain stroke, the stroke volume is very important and therefore it should be optimized. Actually in the case of increased blood current, coronary arteries – that are under pressure- increase the abnormal diastolic aortic pressure leading to increased left ventricular pressure that may leave destructive effects on different organs such as the eyes, brain and kidney. According to the mentioned targets, the cost function is recommended as equation (6):

$$(6) \quad \text{Cost} = \alpha_1 O_{V_I} + \alpha_2 O_{V_E} + \alpha_3 O_{V_F} + \alpha_4 U_{n_I} + \alpha_5 U_{n_E} + \alpha_6 U_{n_F} + \alpha_7 St_I + \alpha_8 St_E + \alpha_9 St_F + \alpha_{10} SV + \alpha_{11} LAP + \alpha_{12} MAP + \alpha_{13} MPS$$

In which (O_{V_I}) , (O_{V_E}) , (O_{V_F}) are overshoot in isovolumic, ejection and filling modes respectively. (U_{n_I}) , (U_{n_E}) , (U_{n_F}) are defined as undershoot in isovolumic, ejection and filling situations, and (St_I) , (St_E) , (St_F) are denoted the settling of these three modes. (SV) denotes the stroke volume, (LAP) is left atrial pressure, (MAP) is defined the minimum aortic pressure and (MPS) is the mean pump speed. According to the importance of the minimization of overshoot, undershoot and settling time, the coefficients α_1 - α_9 are chosen accordingly. The coefficients

α_{10} - α_{13} are selected as it is defined in [12]. Considering to cost function, illustrated in (6) and the system dynamic equations denoted in (1) – (5), there is a bounded optimizations problem that is solved by intelligent optimization algorithms.

4. Calculation of the maximum acceptable range of uncertain parameters

In this section, we find the uncertainties range by classifying the parameter uncertainties in two different group of multiplicative and additive one. Then for such predefined structures the stabilizer feedback controller is designed. Without loose of generality in this paper, we considers the uncertainty in a single parameter that may be generalized to multi-parameters without losing the generalization.

Consider a system with the following structure:

$$(7) \quad \dot{P} = AP + \Delta_1 P + C + \Delta_2 + u$$

Where Δ_2 and Δ_1 are the additive and multiplicative uncertainty, respectively. According to Section 3 in this paper we just consider the R^* uncertainty but without loose of generality the proposed method can be applied for other uncertain parameters similarly. Adding uncertainty to R^* in equation (3) R^* will be written as:

$$(8) \quad R^* = \bar{R}_t + \Delta_{R_t} + \bar{R}_o + \Delta_{R_o} + \bar{R}_p + \Delta_{R_p} + \bar{R}_{su} + \Delta_{R_{su}}$$

Equation (8) is summarized as equation (9):

$$(9) \quad R^* = \bar{R} + \Delta_{R^*}$$

Where \bar{R} is the nominal value of R^* and the uncertain part of R^* is expressed by Δ_{R^*} .

Substituting R^* in equation (1) with (8), one can calculated A and C and Δ_1 and Δ_2 in equation

$$(7). (\Delta_1 = \Delta_{R^*}, \Delta_2 = 0)$$

4.1. Problem definition

In this section we present two cases, the uncertainty band for the changes we make to ensure sustainability. These lemmas are presented for multiplicative and additive uncertainties, since the model parameters uncertainties may have both structures. However according to the fact that the present paper only considers the uncertainty in R^* , the structure under study in the simulation would be of the additive one.

Theorem 1: Consider a non-linear system described by equations (10) and (11) and assume the non-deterministic functions of f_1 and f_2 denoted as the bounded multiplicative and additive uncertainties where β_1 and β_2 define the upper bound of f_1 and f_2 norms.

$$(10) \quad \dot{P} = AP + B_1 f_1(P(t), t) + B_2 u + f_2(t)$$

$$(11) \quad Z(t) = CP(t) + Du(t)$$

$$(12) \quad \|f_1(P(t), t)\| \leq \beta_1 \|P(t)\|; \|f_2(t)\| \leq \beta_2$$

And it is convenient to make the following assumptions on the system matrices $D^T D$ is nonsingular and $D^T C = 0$, then a controller $u(t) = kp(t)$ is found that guarantees lyapunov stability, decrease disturbances output gain and find the maximum allowable bound of uncertainty (proof: see [12]).

4.1.1. Dealing with the uncertainty of the additive uncertainty when multiplicative uncertainty is negligible

If one can ignore the multiplicative uncertainty, Δ_1 in equation (7) could be omitted and the equations (10) to (11) would be expressed as (13) and (14).

$$(13) \quad \dot{P} = AP(t) + B_2 u(t) + f_2(t)$$

$$(14) \quad Z(t) = CP(t) + Du(t)$$

Theorem 2: consider system (13) holds. Then there exists a state feedback controller $u(t)$ such

that $T_{f_2} \leq \gamma (T_{f_2}$ is f_2 output gain) if and only if there exists a positive (semi) definite solution for algebraic equation (15) such that matrix (16) be stable (all eigenvalues have negative real part)

$$(15) \quad A^T P + P A - P B_2 (D^T D)^{-1} B_2^T P + \gamma^{-2} P^T P + C^T C = 0$$

$$(16) \quad A - B_2 (D^T D)^{-1} B_2^T P + \gamma^{-2} P$$

And the feedback controller is as follows (proof: see [13]):

$$(17) \quad u(t) = kP(t)$$

$$(18) \quad k = -(D^T D)^{-1} B_2^T P$$

4.1.2. Multiplicative uncertainty when dealing with the uncertainty of the additive to ignore

In this section, the maximum uncertainty range within which the close loop system remains stable is examined. In this case, the multiplicative uncertainty Δ_2 is ignored and the relations are expressed as equations (19) and (20).

$$(19) \quad \dot{P}(t) = AP(t) + f_1(P(t), t) + B_2 u(t)$$

$$(20) \quad Z(t) = CP(t) + Du(t)$$

$$(21) \quad \|f_1(P(t), t)\| \leq \beta_1 \|P(t)\|$$

Theorem 3: for $\alpha \in \mathbb{R}^+$, Suppose:

$$(22) \quad \beta_1 \leq \frac{\alpha}{2\|Q\|}$$

And let symmetric positive definite matrix Q be the solution of Riccati equation (23):

$$(23) \quad A^T Q + QA + (\alpha + 2)I = 0$$

Then the closed loop system (19) is asymptotically (proof: see [13]). The proposition expressed by the uncertainty of the method is theoretically calculated. In this paper, without loss of generality, multiplicative uncertainty is considered.

4.2. Description of the LVAD system with multiplicative uncertainty

The system described in section 3 is expressed in terms of and the B_1 range is founded by theorem 3 and the calculated B will be compared by the uncertainty bound which is defined by simulation results. The controller $u(t)$, in this paper, is calculated based on GA and PSO methods.

Apply uncertainty the LVAD system of (19) is expressed as equation (24):

$$(24) \quad \dot{P} = \begin{bmatrix} \frac{-b(t)}{c(t)} & 0 & 0 & 0 & 0 & \frac{-1}{c(t)} \\ 0 & \frac{-1}{R_2 C_R} & \frac{1}{R_2 C_R} & 0 & 0 & 0 \\ 0 & \frac{1}{R_2 C_R} & \frac{-1}{R_2 C_R} & 0 & \frac{1}{C_R} & 0 \\ 0 & 0 & 0 & 0 & \frac{-1}{C_R} & \frac{1}{C_R} \\ 0 & 0 & \frac{-1}{L_R} & \frac{1}{L_R} & \frac{-R_R}{L_R} & 0 \\ \frac{1}{L^*} & 0 & 0 & \frac{-1}{L^*} & 0 & \frac{-R^*}{-L^*} \end{bmatrix} P + \begin{bmatrix} 0 & 0 & 0 & 0 & 0 & 0 \\ 0 & 0 & 0 & 0 & 0 & 0 \\ 0 & 0 & 0 & 0 & 0 & 0 \\ 0 & 0 & 0 & 0 & 0 & 0 \\ 0 & 0 & 0 & 0 & 0 & 0 \\ 0 & 0 & 0 & 0 & \frac{\Delta_{R^*}}{-L^*} & 0 \end{bmatrix} P + \begin{bmatrix} \frac{1}{c(t)} & \frac{-1}{c(t)} \\ \frac{-1}{R_R} & 0 \\ 0 & 0 \\ 0 & \frac{1}{C_R} \\ 0 & 0 \\ 0 & 0 \end{bmatrix} \begin{bmatrix} \frac{1}{R_{R1}} r(x_2 - x_1) \\ \frac{1}{R_{R2}} r(x_4 - x_3) \end{bmatrix} + \begin{bmatrix} 0 \\ 0 \\ 0 \\ 0 \\ 0 \\ \frac{Y}{I^* r_0} \end{bmatrix} I(t)$$

Lemma 1- for system (24), with the multiplicative uncertainty Δ_{R^*} there exists a stabilizer feedback controller if $|\Delta_{R^*}| \leq 0.01518$ holds.

Proof: comparing equations (19) and (24) leads to the conclusion that $\|f_1\| = \left| \frac{\Delta_{R^*}}{-L^*} x_6 \right|$. On the other hand, we know that $\|P(t)\|_2^2 = \|x_1^2 + x_2^2 + \dots + x_6^2\|$. Now the combination of both equations leads to the conclusion that $\|f_1(P(t), t)\| - \left| \frac{\Delta_{R^*}}{-L^*} x_6 \right| \leq \beta_1 \|x_1^2 + x_2^2 + \dots + x_6^2\|$. Therefore equation (21) holds. So according to the Theorem 3, there is a stabilizer feedback controller for this system. It should be noted that the β value which is calculated for LVAD system through theorem 3 is equal to 0.01518.

5. Determination of the stability range of the uncertain parameters

After calculating the control parameters of the genetic algorithm and particle swarm, the allowable rang of uncertain parameters is determined and compared with the β_1 value obtained from Lemma 1. However, the resistance of the control parameter changes in the controller design

algorithm is compared to PSO and GA.

5.1. Using genetic algorithms to design the optimal controller

GA is a population based optimization technique which has same advantages such solving bad behavior optimization problems which hardly relative to parameters changes, the fast speed of searching the large spaces, parallel processing which raises the convergence rate. This algorithm can be divided into three modes: A) Reproduction: the greatest individuals of the existing population are selected to generate the next population. B) Cross-over: some couples are selected from the population to be integrated with each other and exchange the genetic informations. C) Mutation: the genetic informations of individuals are changed according to special probability rules to enlarge the searching region. The GA structure is shown in Figure 3. The blending method is used to combine the populations [15].

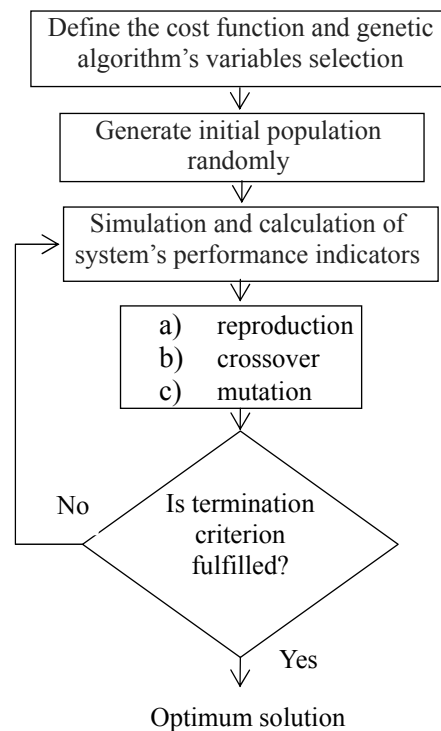


Figure 3- GA flowchart.

Parameters used in the GA for the LVAD is observed in Table (4).

5.2. Particle Swarm Optimization algorithm for controller design

Particle swarm optimization algorithm is a population-based optimization method which was proposed firstly by Kennedy and Eberhart [16]. Ease of implementation and high speed are advantages of PSO, such as genetic algorithms are evolutionary Dygrrvsh. In recent years a variety of topologies for PSO algorithm is proposed such as circular, star and square structures [17]. In D-dimensional search space best position of particle is denoted by $p_i = (p_{i1}, p_{i2}, \dots, p_{iD})$ and the best position of group is illustrated by $g = (g_1, g_2, \dots, g_D)$. In the final equation of particle speed is defined as follows:

$$(25) \quad v_{id}(t+1) = \omega v_{id}(t) + c_1 \text{rand}_1(p_{id}(t) - x_{id}(t)) + c_2 \text{rand}_2(g_{id}(t) - x_{id}(t))$$

The group particles move from the previous position toward the new one according to equation (26):

$$(26) \quad x(t+1) = x(t) + v(t+1)$$

In equation (25), ω is the particle's inertia coefficient and c_1 and c_2 are Hook's elastic coefficients which are usually defined by 2. In order to randomize the speed identity, these coefficients, i.e. c_1 and c_2 are multiplied by rand_1 and rand_2 . In the implementation of PSO, the value of ω is usually decreases as a line from 1 to near zero. In general, the inertia coefficient ω is set as equation (27) [18].

$$(27) \quad \omega = \omega_{\max} - \frac{\omega_{\max} - \omega_{\min}}{\text{iter}_{\max}} \cdot \text{iter}$$

In equation (27), iter_{\max} is the iteration number, iter is the current iteration number, ω_{\max} and ω_{\min} are the maximum and minimum inertia coefficients, respectively. Figure (4) shows the PSO flowchart.

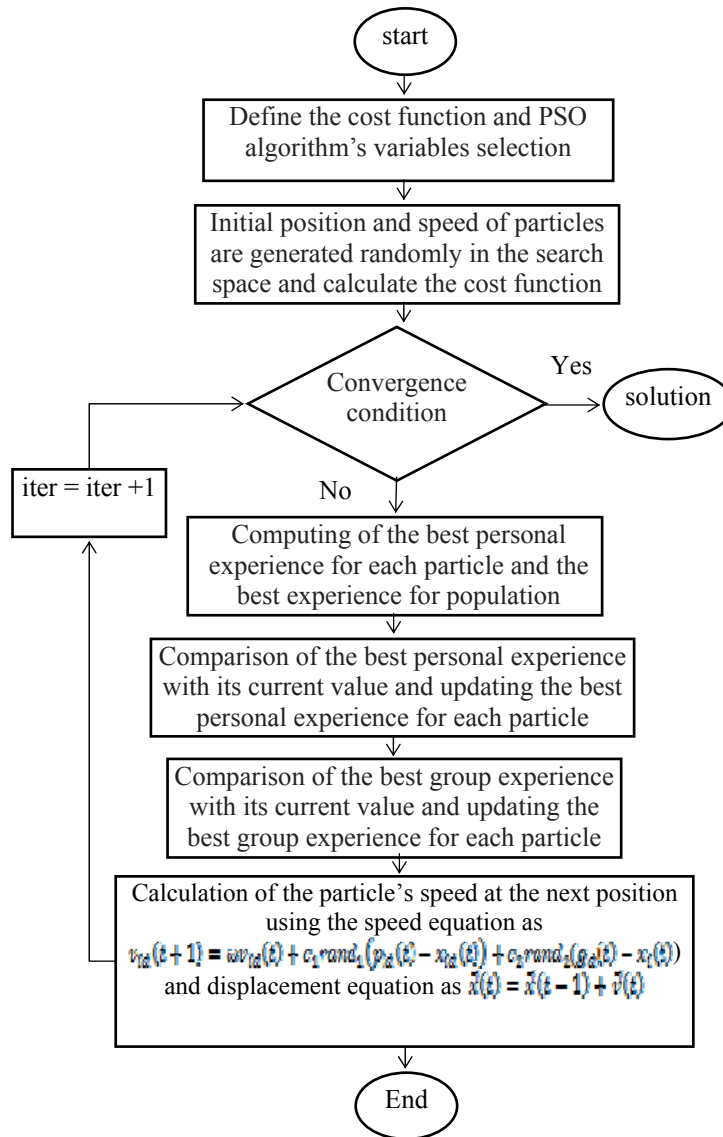


Figure 4. Particle Swarm Algorithm Flowchart.

The parameters used in PSO for the LVAD problem are observed in table (4).

6. Calculation of the uncertain parameters stability range

In this section, we simulate the system of figure 2 [10]. In Table 4 Parameters of two intelligent algorithms are shown.

Table 4 - Algorithms Parameters

	parameter	value
GA Algorithm	Number of the initial population	20
	Percent of regeneration	50
	Percent of mutation	20
	Number of iterations	20
PSO Algorithm	Number of the initial population	20
	w	0.9
	C ₁ ,C ₂	2
	Number of generation iterations	20

The best value of cost function obtained from GA and PSO are 250.68 and 238.22, respectively. The best improvement is related to PSO, which has the lower cost in compare with GA. We place the optimal value of parameters in system's equations. Using these parameters and according to equation (1), the optimal value of feedback gain k is obtained by LQR instruction. The region of Δ_{R^*} venation is shown by varmin and varmax which illustrates the maximum and minimum allowable values of R^* which remains the stability. For example in isovolumic, in other word we should mention that if the R^* value changes from $\bar{R}^* - \text{varmin}$ to $\bar{R}^* + \text{varmax}$ the controlling gain which is obtained through optimization method can stabilize the LVAD system. As an example the value of varmin and varmax in isovolumic, ejection and filling states in absence of controller are -0.01 and 0.1 respectively. So we come to the conclusion that the actual allowable bound for R^* variation from nominal value is 0.01 which is approximately equal to 0.01518 obtained from lemma 1 previously. As it is show in figure 5 system is so sensitive to R^* variation and by changing the nominal value system show oscillating behavior and by increasing the Δ_{R^*} it becomes unstable. Figure 6 and 7 shows the values of varmin and varmax for controlled systems, where the controller is designed by GA and PSO respectively. As it is mentioned in table (6) the controller obtained by PSO leads to the larger bound of allowable Δ_{R^*} . As it is illustrated in

table (5) both algorithms keep the overshoot on zero level PSO algorithm decreases the undershoot level to -0.0206 which is more effective in compare with GA during isovolumic state. In isovolumic state GA is effectively decreases the settling time in compare with PSO which is 9.3618. As it is mentioned in table (5) the undershoot value in ejection state is similar in both algorithms which is equal to -0.386 PSO algorithm enhances the settling time in compare with GA, but the enhancement value is negligible considering to table (6) are can come to the conclusion that PSO optimal controller is much more robust in compare with the controller designed by GA algorithm.

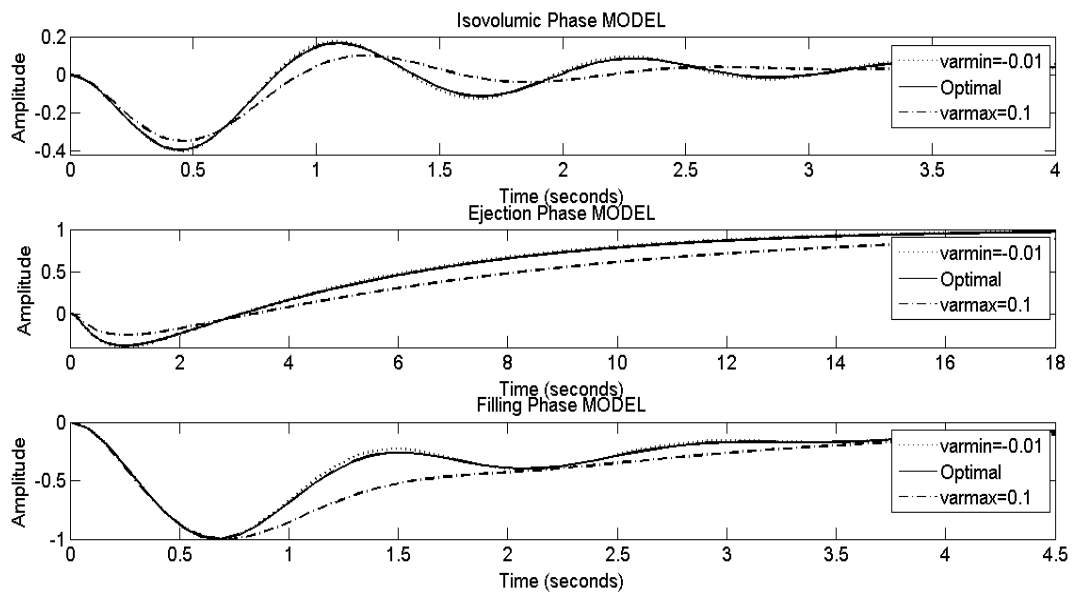


Figure 5: Step response of the model equation (1) for all modes of aortic and mitral uncertainty in the parameter R^* .

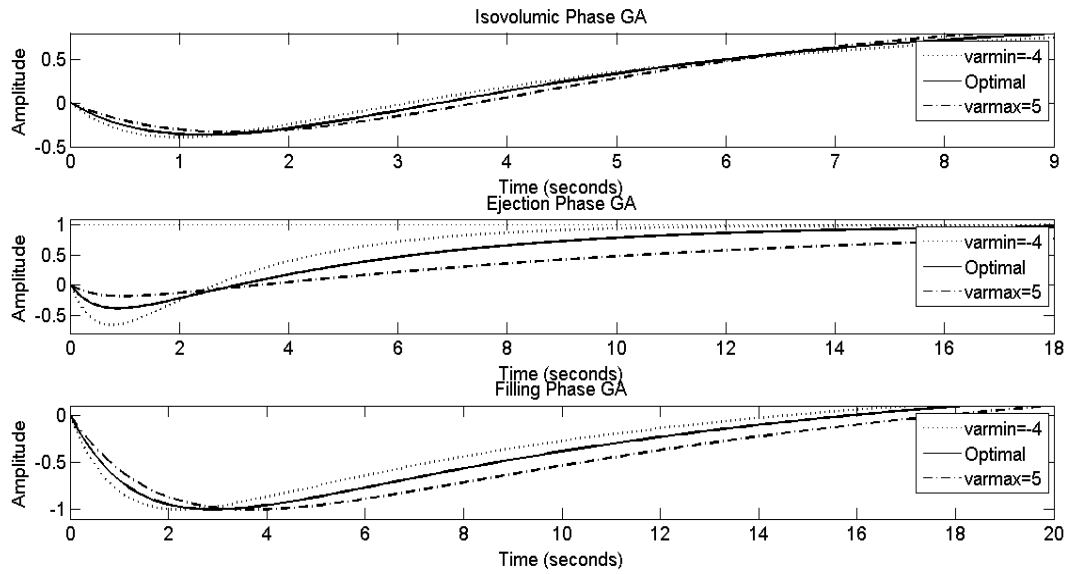


Figure 6: GA algorithm to optimize the step response for all types of aortic and mitral uncertainty in the parameter R^* .

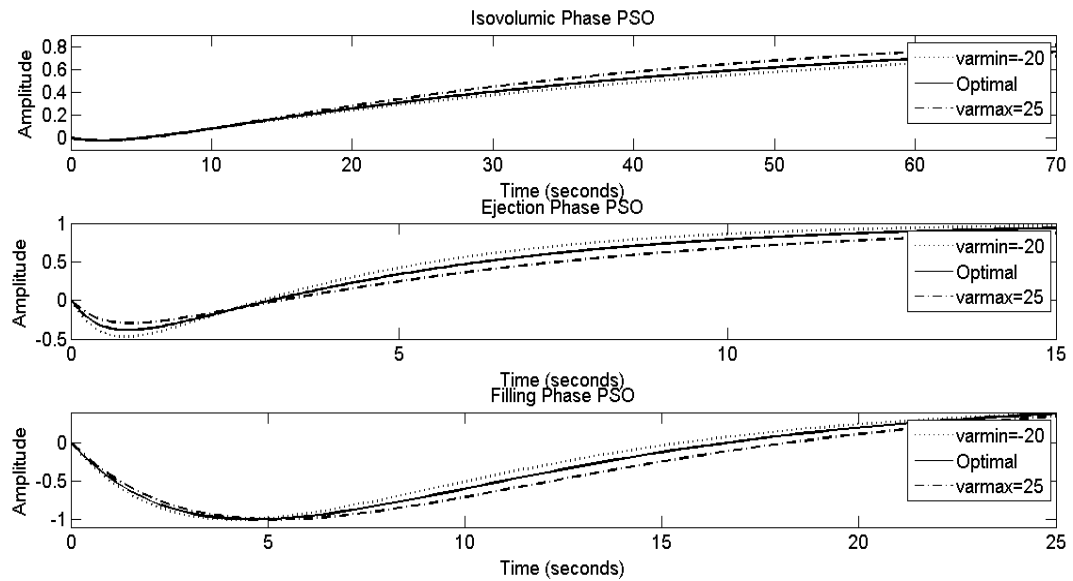


Figure 7: Step response for all types of aortic and mitral PSO algorithm to optimize the uncertainty in the parameter R^* .

Table 5 - Comparison between the two approaches outputs Smart

		Equation (1) model	Genetic Algorithm	Particle Swarm Algorithm
Isovolumic	Overshoot	0	0	0
	Undershoot	-0.396	-0.364	-0.0206
	Settling time	3.7234	9.3618	60.1347
Ejection	Overshoot	0	0	0
	Undershoot	-0.382	-0.386	-0.386
	Settling time	14.7215	15.6077	15.6051
Filling	Overshoot	0	0	0
	Undershoot	-1	-1	-1
	Settling time	4.4291	18.1295	25.2611

Table (6) - R^* parameter range for which the system is stable

Equation (1) model	Isovolumic	$R^* - 0.01 \leq R^* \leq R^* + 0.1$
	Ejection	
	Filling	
Genetic Algorithm	Isovolumic	$R^* - 4 \leq R^* \leq R^* + 5$
	Ejection	
	Filling	
Particle Swarm Algorithm	Isovolumic	$R^* - 20 \leq R^* \leq R^* + 25$
	Ejection	
	Filling	

7. Conclusion

In this paper we define the allowable bound for uncertain parameter's variations. We divide the uncertainties to two main groups of additive and multiplicative structures and find the theoretical stabilizable bound of uncertainty. Then we compare the robustness of two optimal controller designed by PSO and GA algorithms and show that the first one includes larger region of stabilizable uncertain variables. We also compare the transient behaviors of output in three different LVAD modes which are isovolumic, ejection and filling state. In our future work we

will design a robust controller to enlarge the uncertainty bound which keeps the system stable and consider different uncertainties which are related to different biological parameters of system.

References

- [1] Shamsi Afzal and Abbas Ebadi, "Risk Factors of Cardiovascular Diseases in Elderly People," Iranian Journal of Critical Care Nursing, vol. 3, no. 4, pp. 187-192, 2011.
- [2] Fateme Shojaei, "Quality of Life in Patients with Heart Failure," Journal of Faculty of Nursing and Midwifery, vol. 14, no. 2, pp. 5-13, 2008.
- [3] Andre Pohlmann et al., "Drive optimisation of a pulsatile Total Artificial Heart," Archives Of Electrical Engineering, vol. 60, no. 2, pp. 169-178, 2011.
- [4] Wu Yi, Allaire Paul, Tao Gang, and Olsen Don, "Modeling , Estimation and control of Human circulatory system with a Left Ventricular Assist Devices," IEEE Transactions On Control Systems Technology, vol. 15, no. 4, 2007.
- [5] Marian Walter, Stefanie Heinke, Sebastian Schwandtner, and Steffen Leonhardt, "Control Strategies for Mechanical Heart Assist systems," IEEE Multi-Conference on Systems and Control, vol. 1, no. 5, pp. 57-62, 2012.
- [6] Marian Walter, Stefanie Heinke, Sebastian Schwandtner, and Steffen Leonhardt, "Physiological Control of Left Ventricular Assist Devices Based on Gradient of Flow," American Control Conference, vol. 13, no. 4, pp. 3829-3834, 2005.
- [7] Antonio Ferreira, Student Member, and Shaohui Chen, "A Nonlinear State-Space Model of a Combined Cardiovascular System and a Rotary Pump," IEEE Conference on Decision and Control, pp. 897-902, 2005.
- [8] Yi Wu, Paul Allaire, Gang Tao, and Don Olsen, "Modeling, Estimation and Control of Cardiovascular Systems with A Left Ventricular Assist Device," American Control Conference, vol. 13, no. 6, pp. 3841-3846, 2005.
- [9] p He, J Bai, and D.D Xia, "Optimum control of the Hemopump as a left-ventricular assist device," Medical & Biological Engineering & Computing, vol. 43, pp. 136-141, 2005.
- [10] George Faragallah, Yu Wang, Eduardo Divo, and Marwan A Simaan, "A New Current-Based Control Model of the Combined Cardiovascular and Rotary Left Ventricular Assist Device," American Control Conference, pp. 4775-4780, 2011.
- [11] Liu Baoding, Uncertainty Theory. Beijing, China, 2004.
- [12] He p, Bai J, and Xia D.D, "Optimum control of the Hemopump as a left-ventricular assist device," Medical & Biological Engineering & Computing, vol. 43, pp. 136-141, 2005.
- [13] Zhou Kemin, "Robust and optimal control," 1995.
- [14] Toivonen Hannu T, "Lectures on Advanced control," chap 4(the H ∞ Optimal Problem), 1998.
- [15] Haupt R.L and Haupt S.E, "Practical Genetic Algorithms," John Wiley & Sons, 2004.
- [16] Kennedy J and Eberhart R, "Particle Swarm Optimization," IEEE International Conference on Neural Networks, vol. 5, pp. 1942-1948, 1995.
- [17] Kennedy J and Mendes R, "Neighborhood topologies in fully-informed and best-of neighborhood particle swarms," IEEE International Workshop, pp. 45-50, 2003.
- [18] Jin N and Rahmat-Samii Y, "Advances in Particle Swarm Optimization for Antenna Designs: Real-Number, Binary, Single-Objective and Multiobjective Implementations," IEEE Tran, vol. 55, no. 3, pp. 556-567, 2007.